Computers and Mathematics with Applications 64 (2012) 476–488

Contents lists available at SciVerse ScienceDirect

Computers and Mathematics with Applications

journal homepage: www.elsevier.com/locate/camwa

Studying the effects of a longitudinal magnetic field and discrete isoflux heat source size on natural convection inside a tilted sinusoidal corrugated enclosure

Salam Hadi Hussain *, Ahmed Kadhim Hussein, Rehab Noor Mohammed

Mechanical Engineering Department, College of Engineering, Babylon University, Babylon Province, Iraq

ARTICLE INFO

Article history:
Received 13 April 2011
Received in revised form 7 December 2011
Accepted 8 December 2011

Keywords:
Magnetohydrodynamic natural convection
Longitudinal magnetic field
Tilted corrugated enclosure
Isoflux heat source
Finite volume
Hartmann number

ABSTRACT

In the present work, the effects of the longitudinal magnetic field and the heat source size on natural convection heat transfer through a tilted sinusoidal corrugated enclosure for different values of enclosure inclination angles are analyzed and solved numerically by using the finite volume technique based on body fitted control volumes with a collected variable arrangement. A constant heat flux source is discretely embedded at the central part of the bottom wall whereas the remaining parts of the bottom wall and the upper wall are assumed adiabatic, and two vertical sinusoidal corrugated walls are maintained at a constant low temperature. The range of the variable parameters considered in the present analysis is as follows: the enclosure inclination angle is varied from 0° to 135°, the ratio of the size of the heating element to enclosure width varied from 20 to 80% of enclosure reference length, Hartmann number is varied from 0 to 100, and Rayleigh number varied from 10^3 to 10^6. Liquid gallium with constant Prandtl number (0.02) is used as a working fluid with constant properties except the density. The obtained results indicated that streamlines are affected strongly by the magnetic field especially for small values of inclination angle ($\Phi = 0°$) and Rayleigh number ($Ra = 10^3$–10^6). The magnetic field effect decreases with an increase in the enclosure inclination angle ($\Phi > 0°$) especially for large values of Rayleigh number. The increase in Hartmann number will cause the temperature lines to become symmetrical in shape for large values of Rayleigh number ($Ra = 10^5$–10^6). The results also explain that the temperature lines are very little affected by the inclination angle especially for small values of ($\varepsilon = 0.4$) and ($Ra = 10^4$), but this effect will increase especially for ($\varepsilon = 0.8$) and ($Ra = 10^6$). The Nusselt number increases first with an increase in inclination angle ($0° \leq \Phi \leq 45°$), then is slightly affected for ($45° < \Phi \leq 90°$), and finally decreases for ($90° < \Phi \leq 135°$). An empirical correlation is developed by using Nusselt number versus Hartmann and Rayleigh numbers, and enclosure inclination angle. The increase in Hartmann number and the ratio of heating element to enclosure width will decrease the Nusselt number. Furthermore, four mathematical correlations are extracted from the results and presented, which can be used to accurately predict the average Nusselt number in terms of enclosure inclination angle, Hartmann, and Rayleigh numbers.

1. Introduction

The use of longitudinal magnetic field has a significant role in recent years, especially in engineering applications such as magnetic cooling systems, magnetic refrigerators, water treatment devices, corrosion inhibition treatment,

* Corresponding author. Tel.: +964 7802431066.
E-mail addresses: salamphd1974@yahoo.com (S.H. Hussain), ahmedkadhim74@yahoo.com (A.K. Hussein), rehabnoor@gmail.com (R.N. Mohammed).

0898-1221/$ – see front matter © 2011 Elsevier Ltd. All rights reserved.
doi:10.1016/j.camwa.2011.12.022

Nomenclature

B_0	The magnitude of magnetic field (T)
g	The gravitational acceleration (m/s^2)
Gr	Grashof number
k	Thermal conductivity of fluid, (W/m °C)
H	Height of the sinusoidal corrugated enclosure (m)
Ha	Hartmann number
$\underline{Nu}$	Local Nusselt number
$\overline{Nu}$	Average Nusselt number
P	Pressure (N/m^2)
P	The dimensionless Pressure
Pr	Prandtl number
q	Heat flux (W/m^2)
Ra	Rayleigh number
T	Temperature (°C)
T_c	Temperature of the cold surface, (°C)
u	Velocity component along x-axis (m/s)
U	Dimensionless velocity component along x-axis
v	Velocity component along y-axis (m/s)
V	Dimensionless velocity component along y-axis
W	Width of the sinusoidal corrugated enclosure (m)
x	Longitudinal distance in x-direction (m)
X	Dimensionless coordinate along the horizontal axis
y	Longitudinal distance in y-direction (m)
Y	Dimensionless coordinate along the vertical axis

Greek symbols

β	Volumetric coefficient of thermal expansion (1/K)
ε	Ratio of heating element to enclosure width, L/W
θ	The dimensionless temperature
θ_S	Local dimensionless surface temperature
μ	Dynamic viscosity (Pa s)
ν	Kinematics viscosity (m^2/s)
ρ	Density of the working fluid (kg/m^3)
σ_e	The electrical conductivity of fluid (s/m)
Φ	Inclination angle of the enclosure (°)

magnetohydrodynamics (MHD) power generation, plasma techniques and crystal growth [1]. The application of magnetic field to convection processes will play as a control factor in the convection by damping both the flow and temperature oscillations in material manufacturing fields. In several energy conversion processes, strong external magnetic fields are applied to liquid flows. For example, liquid lithium was used to extract energy from fusion reactor and to breed the tritium for fuel the fusing plasma during which liquid lithium must be pumped through strong magnetic field needed to confine the plasma [2]. In manufacturing processes of semi-conductor crystals, the external magnetic field was used to reduce the buoyancy driven fluctuations, and then to modify the interface shape and rate of solidification [3]. Moreover, the magnetic field plays an important role in affecting nucleation, crystal growth, segregation by controlling fluid flow and heat transfer [4]. The convection heat transfer in wavy and sinusoidal wall enclosures without the presence of the magnetic field was studied numerically and experimentally in a great deal of research with different geometries and boundary conditions. Yao [5], Adjlout et al. [6], Wang and Chen, [7], and Metwally and Manglik [8] concluded numerically that the wavy or sinusoidal walls were very effective on the flow and heat transfer rate, and the average heat transfer with the surface waviness decreased when compared with flat wall cavity, while Kruse and Von Rohr [9] examined the flow over a heated sinusoidal wavy wall experimentally. The effect of the Nusselt number on the flow inside the wavy enclosures was studied by Chen et al. [10]. From the other hand, the effect of the important geometric parameters of the wavy enclosure on the convection heat transfer and flow without the existence of the magnetic field was discussed in a great deal of previous research. The effect of the aspect ratio on the convection heat transfer and fluid flow through wavy channels was studied by Comini et al. [11]. Das and Mahmud [12] showed that the amplitude–wavelength on the natural convection affected local heat transfer rate. On the other hand, Dalal and Das [13] explained that the undulation in the right wall of the enclosure affected local heat transfer rate and flow field as well as thermal field. The inclination angle variation of the enclosure was a very important object, and there are no sufficient research that studied this object in detail. Varol and Oztop [14]

studied the effect of inclination angle on heat transfer and fluid flow without the presence of the magnetic field in a wavy enclosure. They concluded that the inclination angle was the most important and effective parameter on the heat transfer which can be used to control the heat transfer inside the enclosure. Very recently, Hussain and Mohammed [15] explained that the effects of the out of phase and the inclination angle variations in natural convection through a sinusoidal corrugated enclosure without the presence of magnetic field were very important. The effect of the transverse magnetic field on the two dimensional laminar flow through a square enclosure with isothermal vertical walls and adiabatic horizontal walls was analyzed by Al-Najem et al. [16]. They showed that the suppression effect of the magnetic field on fluid and heat transfer was more significant for low inclination angles and high Grashof numbers. Two-dimensional turbulent flow through square enclosure with differently heated vertical sidewalls was analyzed numerically by Jalil and Al-Tae'y [1]. They explained that the magnetic field in the x-direction was more effective on the flow and thermal fields than in the y-direction. The natural convection in a square cavity filled with an electrically conducting fluid in the presence of external magnetic field parallel to gravity was analyzed by Kandaswamy et al. [17]. Their results explained that for sufficiently large magnetic field ($\mathrm{Ha} = 100$) the convective mode of heat transfer was converted into conductive mode especially in the low region of Grashof number. Pirmohammadi et al. [18] showed that the heat transfer and flow field inside the square enclosure depended strongly on both the strength of the magnetic field and Rayleigh number, and the magnetic field decreased the average Nusselt number. The applying of magnetic field perpendicularly to the hot wall of a three dimensional cubic cavity with different temperatures vertical walls produced the strongest damping effect [19]. The influence of uniform magnetic field on three dimensional turbulent convection heat transfer ($\mathrm{Ra} = 10^8$) was examined by Jalil et al. [20]. Their results showed that the applying of magnetic field in x-direction was more effective than in the y-direction, and the effect of the magnetic field in z-direction occurred between the effects of x- and y-directions respectively. The enclosure inclination angle was considered one of important parameters in the study of the natural convection heat transfer and flow field inside the enclosure with the presence of the magnetic field [21]. They concluded that the average heat transfer rates varied with the angle of inclination due to the change in the total net acceleration of gravitational and magnetizing forces. Laminar free convection inside a square enclosure that was heated from below and cooled from the top while other walls were considered adiabatic was analyzed numerically by Pirmohammadi and Ghassemi [22]. They concluded that the value of Nusselt number depended clearly upon the inclination angle for small values of Hartmann number.

Very recently, Saha [23] used finite element method to solve the steady magneto-convection problem in a sinusoidal corrugated enclosure filled with air as the working fluid. The enclosure under study consisted of two vertical sidewalls at a constant cold temperatures while a constant flux heat source was discretely embedded at the bottom wall, and the remaining parts of the bottom surface and the upper wall were considered to be adiabatic. The uniform external magnetic field (B_0), was applied parallel to the gravity which acted vertically downward. He varied the ratio of the size of the heating element to the enclosure width (ε) from (0.2 to 0.8), Grashof number (Gr) from (10^3 to 10^6), Hartmann number (Ha) from (0 to 100) while the Prandtl number (Pr) was taken as (0.71). He concluded that the increasing of Grashof number largely affected on the streamlines and isotherms especially for ($\mathrm{Ha} = 0$), and this effect decreased with increasing Hartmann number and the ratio of the size of the heating element to the enclosure width.

The aim of the present research is to analyze numerically the effect of longitudinal magnetic field and size of the heat source on natural convection through sinusoidal corrugated enclosure for various values of enclosure inclination angles. The enclosure consists of sinusoidal corrugated vertical side walls and insulated straight horizontal walls except heat source region. The current model is based on the geometry of Saha [23] but in his work attention has been directed toward the problem of magnetoconvection of flow and heat transfer in a sinusoidal corrugated enclosure filled with air as the working fluid and the uniform external magnetic field (B_0) was applied parallel to the gravity. The present work deals with the same geometry but it develops the Saha work [23] by studying the effect of enclosure inclination angle with the presence of a longitudinal magnetic field on the natural convection in a sinusoidal corrugated enclosure filled with liquid gallium ($Pr = 0.02$) rather than air ($Pr = 0.71$) as the working fluid. A wide range of dimensionless variables are examined here: ($\mathrm{Ha} = 0$–100), ($\mathrm{Ra} = 10^3$–10^6), ($\varepsilon = 0.2$–0.8) and ($\Phi = 0^\circ$–135°). Finite volume technique instead of finite element method is used to solve the governing equations of the present work.

2. Problem formulation and mathematical model

The physical model considered here is shown in Fig. 1, along with the important geometric parameters. A Cartesian coordinate is used with origin at the lower left corner of the computational domain. It consists of a sinusoidal corrugated enclosure of dimensions, ($W \times H$). In this work, two sidewalls are maintained at a constant low temperature (T_c), and a constant flux heat source (q), is discretely embedded at the bottom wall, while the remaining parts of the bottom wall and the upper wall are considered to be thermally insulated. The enclosure has the same height and width, $H = W$ with single corrugation frequency along the sidewalls and the corrugation amplitude has been taken fixed at 10% of the enclosure length. The shape of the wavy vertical sidewalls is taken as sinusoidal. The effect of different inclination angles on the heat transfer process inside the sinusoidal corrugated enclosure is studied in the present work. Inclination angle (Φ) of the enclosure with the horizontal is varied from (0° to 135°) in steps of 45°. The ratio of the size of the heating element to the enclosure width, is varied as ($\varepsilon = 0.2$–0.8), Hartmann number is varied from (0 to 100), Rayleigh number for all cases studied have been varied from (10^3 to 10^6). The enclosure is filled with liquid gallium whose Prandtl number is fixed to be 0.02. The velocity and temperature fields inside the enclosure are presented in terms of a streamline and an isotherm maps and the

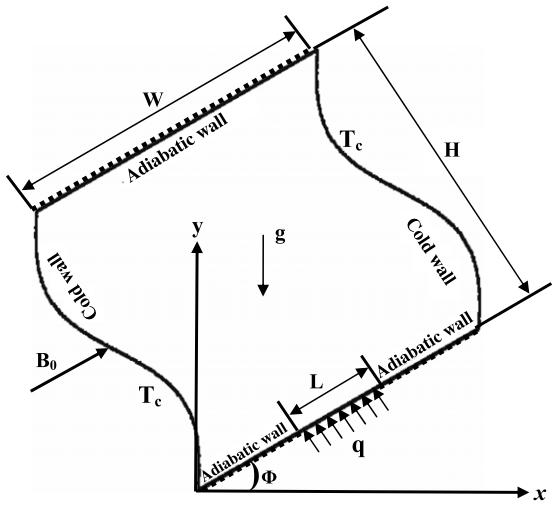

Fig. 1. Schematic configuration of the tilted sinusoidal corrugated enclosure with coordinate system along with boundary conditions and longitudinal magnetic effect.

effects of the magnetic field strength on transport phenomenon are determined. The fluid properties are also assumed to be constant, except for the density in the buoyancy term, which follows the Boussinesq approximation. The fluid within the enclosure is assumed Newtonian while the effect of viscous dissipation, radiation and Joule heating are neglected. The viscous incompressible flow and the temperature distribution inside the enclosure are described by using the Navier–Stokes and energy equations, respectively. The governing equations are transformed into a dimensionless form under the following non-dimensional variables [23]:

$$\theta = \frac{T - T_c}{\Delta T}, \quad X = \frac{x}{H}, \quad Y = \frac{y}{H}, \quad U = \frac{uH}{\alpha}, \quad V = \frac{vH}{\alpha}, \quad P = \frac{pH^2}{\rho\alpha^2},$$
$$\Delta T = \frac{qW}{k}, \quad Pr = \frac{\upsilon}{\alpha}, \quad \mathrm{Ra} = \frac{g\beta\Delta TH^3Pr}{\upsilon^2} \tag{1}$$

where X and Y are the non-dimensional coordinates measured along the horizontal and vertical axes, respectively, U and V being the dimensionless velocity components along X and Y axes. The non-dimensional forms of the governing equations under steady state condition are expressed in the following forms [24]:

$$\frac{\partial U}{\partial X} + \frac{\partial V}{\partial Y} = 0 \tag{2}$$

$$U\frac{\partial U}{\partial X} + V\frac{\partial U}{\partial Y} = -\frac{\partial P}{\partial X} + \mathrm{Pr}\left(\frac{\partial^2 U}{\partial X^2} + \frac{\partial^2 U}{\partial Y^2}\right) + \left(\mathrm{Ra}Pr\theta - \mathrm{Ha}^2\,\mathrm{Pr}\,V\right)\sin(\Phi) \tag{3}$$

$$U\frac{\partial V}{\partial X} + V\frac{\partial V}{\partial Y} = -\frac{\partial P}{\partial Y} + \mathrm{Pr}\left(\frac{\partial^2 V}{\partial X^2} + \frac{\partial^2 V}{\partial Y^2}\right) + \left(\mathrm{Ra}Pr\theta - \mathrm{Ha}^2\,\mathrm{Pr}\,V\right)\cos(\Phi) \tag{4}$$

$$U\frac{\partial \theta}{\partial X} + V\frac{\partial \theta}{\partial Y} = \left(\frac{\partial^2 \theta}{\partial X^2} + \frac{\partial^2 \theta}{\partial Y^2}\right). \tag{5}$$

The longitudinal magnetic field effect is inserted into the equation of motion (4) through Hartmann number. The Hartmann number (Ha) is defined as:

$$\mathrm{Ha} = B_0 H\sqrt{\frac{\sigma_e}{\rho\nu}} \tag{6}$$

where B_0 is the magnitude of magnetic field and σ_e is the electrical conductivity. Non-dimensional forms of the boundary conditions for the present problem are specified as follows:

All walls: $U = 0, V = 0$.
Top wall: $\frac{\partial\theta}{\partial Y} = 0$.
Right and left sidewalls: $\theta = 0$.
Bottom wall:

$$\frac{\partial\theta}{\partial Y} = \begin{cases} 0 & \text{for } 0 < X < 0.5\,(1-\varepsilon) \text{ and } 0.5\,(1+\varepsilon) < X < 1 \\ -1 & \text{for } 0.5\,(1-\varepsilon) \le X \le 0.5\,(1+\varepsilon)\,. \end{cases}$$

The average Nusselt number ($\overline{Nu}$) at the heated surface can be written as [25]:

$$\overline{Nu} = \frac{1}{\varepsilon}\int_0^{\varepsilon} \frac{1}{\theta_S}(X)dX \tag{7}$$

where $\theta_S(X)$ is the local dimensionless temperature distribution of the heated surface.

3. Numerical simulation

A FVM (finite volume method) is used to obtain numerical solution of the complete governing Eqs. (2)–(5) on a collocated grid system [26]. Body fitted, non-orthogonal grids are used. The grid generation calculation is based on curvilinear coordinate system applied to fluid flow as described by Thompson et al. [27]. Grids are oriented in such a way that the number of control volumes is higher near the walls where higher gradients of variable values are expected. Two dimensions body fitting grid are used for the present computation. The 2-D computational grids are clustered toward the walls. The location of the nodes is calculated using a stretching function as described by Thompson et al. [27], so that the node density is higher near the flat, wavy walls and the round corners of the sinusoidal corrugated enclosure. More details about grid generation procedure can be found in literature [27]. In the course of discretization, the power scheme and a second-order upwind scheme are respectively utilized for the convection and diffusion terms respectively. The SIMPLE algorithm is selected to solve numerically governing differential equations in their primitive forms. The pressure correction equation is derived from the continuity equation to introduce the local mass balance [26]. The source terms in the governing transport equations are not functions of the respective transport variables and are calculated explicitly. Linear interpolation and numerical differentiation [26] are used to express the cell-face value of variables and their derivatives through the nodal values. Discretized momentum equations lead to algebraic equation systems for velocity components U and V where pressure, temperature, fluid properties are taken from the previous iteration step except the first iteration where initial conditions are applied. These linear equation systems are solved iteratively (inner iteration) to obtain an improved estimate of velocity. The improved velocity field is then used to estimate new mass fluxes, which satisfy the continuity equation. The pressure-correction equation is then solved using the same linear equation solver and to the same tolerance. The energy equation is then solved in the same approach to obtain a better estimate of the new solution. Solutions are assumed to converge when the following convergence criterion is satisfied for every dependent variable at each point in the solution domain:-

$$\frac{\sum_i \sum_j \left|\Phi_{i,j}^{\text{new}} - \Phi_{i,j}^{\text{old}}\right|}{\sum_i \sum_j \left|\Phi_{i,j}^{\text{new}}\right|} \leq 10^{-6} \tag{8}$$

where Φ refers for dependent variables U, V, P, and θ. In this study the SIP-solver based on lower–upper decomposition (ILU) [28,29] is used to solve the linear equation systems. To avoid divergence, an under-relaxation parameter of 0.55 is used for velocity, 0.2 for pressure and 0.85 for temperature.

4. Grid testing

In order to get grid independent solution, a grid testing is performed for a sinusoidal corrugated enclosure with the horizontal flat walls while the shape of the wavy vertical walls is taken as sinusoidal. The enclosure has the same height and width, $H = W$ with single corrugation frequency along the side walls and the corrugation amplitude has been fixed at 10% of the enclosure length. In order to test grid independence of the present solution scheme, many numerical runs are performed for higher Rayleigh number and the same boundary conditions of the current study with $\text{Ra} = 10^6$, $Pr = 0.02$, $\text{Ha} = 100$ and $\Phi = 45^\circ$. In the present work, eight combinations (40×40, 50×50, 60×60, 70×70, 80×80, 100×100, 120×120 and 150×150) of non-uniform grids are used to test the effect of grid size on the predicted results accuracy. Fig. 2 shows the convergence of the average Nusselt number ($\overline{Nu}$), at the heated surface of the sinusoidal corrugated enclosure with grid refinement. It is observed that grid independence is satisfied with combination of (100×100) control volumes where there is insignificant change in the average Nusselt number ($\overline{Nu}$) with the improvement of finer grid. The agreement is found to be excellent which verifies the present calculations indirectly.

5. Verification of numerical results

In order to prove that the present work program is free of error and works very well, a verification test is carried. The present numerical approach is verified against the results published by Pirmohammadi and Ghassemi [22] for natural convection flows with the presence of a longitudinal magnetic field in a tilted square cavity of dimensions ($L \times L$) that was heated from below and cooled from the top while other walls were adiabatic. Fig. 3 shows the streamlines and isotherms calculated by Pirmohammadi and Ghassemi [22] with corresponding streamlines and isotherms computed in the present study for $\text{Ra} = 10^5$, $Pr = 0.02$, Φ changing from 0°, 45°, 90° to 135° and Hartmann numbers ($\text{Ha} = 0$, 50 and 70) using the same boundary conditions with different numerical solver. Excellent agreement is achieved between Pirmohammadi

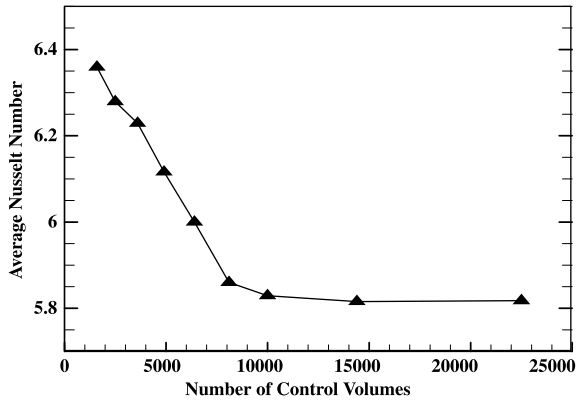

Fig. 2. Convergence of average Nusselt number along the heated bottom wall with grid refinement at Ra $= 10^6$, Ha $= 100$, $Pr = 0.02$, $\varepsilon = 0.8$ and $\Phi = 45°$.

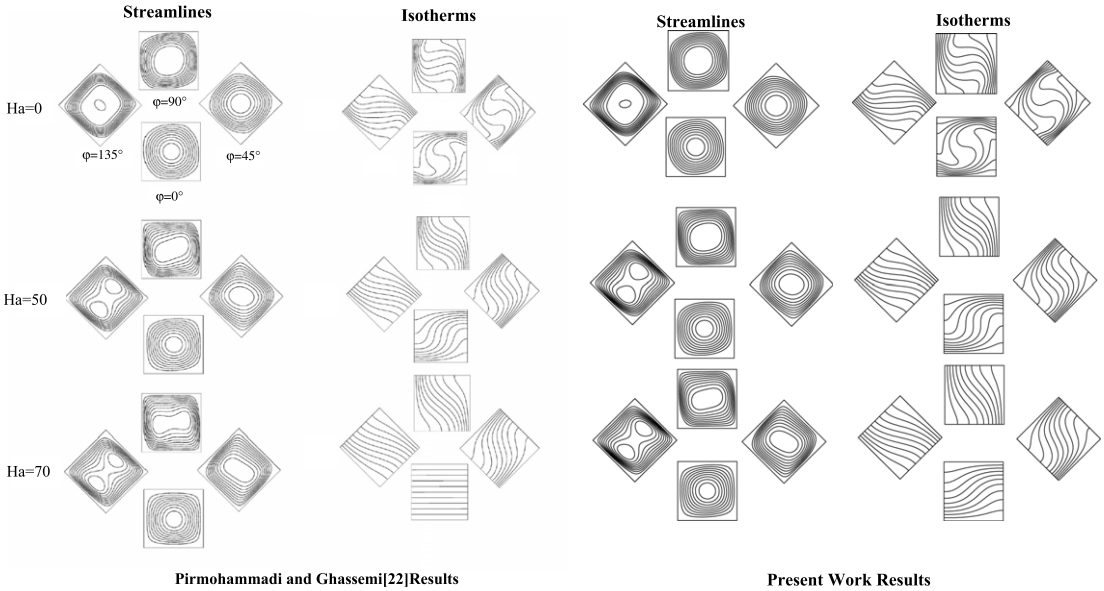

Fig. 3. Comparison of the streamlines and isotherms versus inclination angles and Hartmann numbers between the present work (on the right) and that of Pirmohammadi and Ghassemi [22] (on the left) in a square enclosure filled with liquid gallium using the flow conditions ($Pr = 0.02$, Ra $= 10^5$).

and Ghassemi [22] results and results of present numerical scheme for both streamlines and temperature contours inside a tilted square cavity as shown in Fig. 3. This verification gives a good interest in the present numerical model to deal with the current considered case.

6. Results and discussion

The longitudinal magnetic field and isoflux heat source size effects on the natural convection inside a tilted sinusoidal enclosure for various values of enclosure inclination angles are investigated numerically and the results are plotted for the following ranges: Hartmann numbers (0, 25, 50, 75 and 100), Rayleigh numbers (10^3, 10^4, 10^5 and 10^6), the ratio of the size of the heating element to the enclosure width, is varied as ($\varepsilon = 0.2$, 0.4, 0.5, 0.6, 0.7 and 0.8) and for inclination angles ($\Phi = 0°$, 45°, 90° and 135°). These effects are discussed and presented for both streamlines and isotherms. For streamlines (Fig. 4), at $\varepsilon = 0.2$, $\Phi = 0°$ and Ha $= 0$ and low values of Rayleigh number (10^3–10^4), two large vortices which appear on the left and right sides of the enclosure. Because of the symmetrical boundary conditions about Y-axis, the two large vortices that control the flow field inside a tilted sinusoidal enclosure are symmetrical about the vertical axis (Y-axis) of the enclosure.

The phenomena of the creating of two large vortices inside the enclosure can be described as follows: firstly, the natural convection flow rises upward due to temperature difference along the vertical axis (Y-axis) into the top adiabatic wall. After hitting this latter wall, the flow field changes its direction toward the left and right isothermal vertical cold walls, then the flow passes downwards along the corrugated sinusoidal sidewalls and then horizontally returns to the core region of

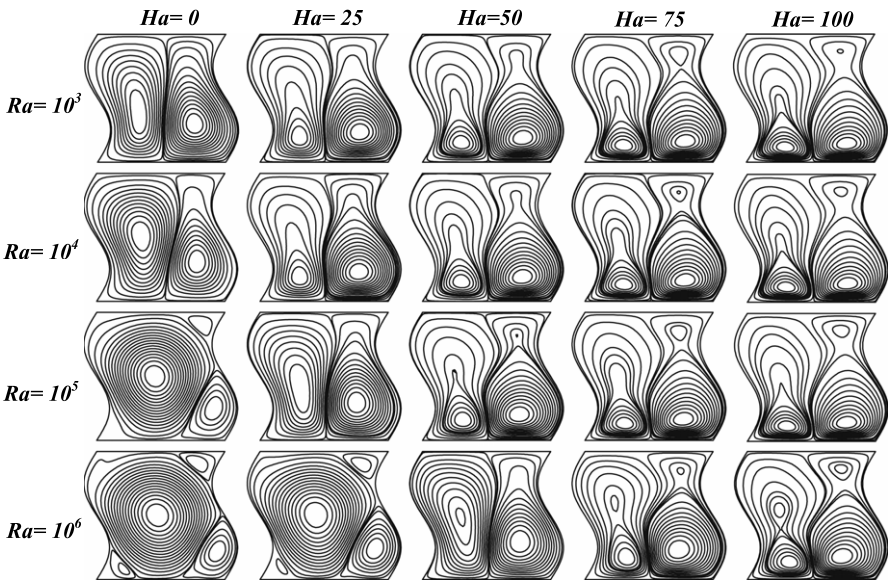

Fig. 4. Streamlines for different Hartmann numbers (Ha) and Rayleigh numbers (Ra) with $\varepsilon = 0.2$ and $\Phi = 0^\circ$.

sinusoidal enclosure after impact the bottom wall. Thus, the flowing fluid is the main reason for creating the two symmetrical large vortices which rotate in opposite directions inside the enclosure. Also, at Ha $=$ 0 and low values of Rayleigh number (Ra $=$ 10^3–10^4), the left vortex core region takes an elliptical shape while right vortices core region takes a circular shape according to the vertical axis of the enclosure. The reason of this behavior, because the viscous forces are stronger than the buoyancy forces and then the heat is transferred by conduction only. Moreover, streamlines shape takes to approach the enclosure geometry. When Rayleigh number increases (Ra $=$ 10^5–10^6), a clear change can be observed in the shape of vortices and only a large vortex can be detected which controls the flow field inside the enclosure. The left vortex controls the flow field inside the enclosure while the right vortex is reduced in size and becomes more smaller and divided into two secondary vortices located near the top and bottom of the right vertical wall, a similar behavior is noticed by Saha [23]. After that, the left vortex begins to spread inside a tilted sinusoidal enclosure causing a high flow field recirculation. The large spread of the left vortex inside the enclosure reduces clearly the right vortex at the right vertical sidewall. This behavior appears due to large increase in the convective effect through the enclosure. The increase in the Hartmann number (Ha $=$ 0–25), does not have a clear effect on the streamlines shape, because the viscous forces are more effective than the buoyancy forces and the heat transfer is due to conduction. Again, streamlines shape takes to approach the enclosure geometry. Further increase in the Hartmann number from (Ha $=$ 50–100) will reduce the convection heat transfer effect and decreases the flow velocity through the enclosure. This phenomena is called flow field damping which was observed by Jalil et al. [20]. For large Rayleigh number, the major vortices spread faster inside the enclosure and divide into small minor vortices in the top and bottom walls. The major vortices that control the flow field located near the bottom wall (see Fig. 4). This behavior due to increase the buoyancy forces role which leads to increase the convection heat transfer effect. In this figure, also it is observed that the vortices centers begin to shift from the enclosure center toward the bottom wall where the heat source exists. When the magnetic field is affected in X-direction, the electromagnetic force will appear in the Y-equations only. For isothermal lines (Fig. 5) at $\varepsilon = 0.2, \Phi = 0^\circ$, Ha $=$ 0 and low values of Rayleigh number (Ra $=$ 10^3–10^4), the increase in the Hartmann number does not have a significant effect on the isothermal lines especially at low value of Rayleigh number. This is because the configuration has a symmetrical boundary conditions and the viscous forces are greater than the buoyancy forces. For large values of Rayleigh number (Ra $=$ 10^5–10^6), the increase in the Hartmann number causes isothermal lines to shift toward the vertical isothermal sidewalls and they divide into two similar contour lines. This is due to increase in the magnetic field which damps the temperature oscillation making the thermal energy to transfer easier through the corrugated cold sidewalls. Also, in this case the conduction effect through the enclosure is high. The streamlines are plotted in Figs. 6, 8 and 10, for different values of Hartmann number (Ha $=$ 0, 25, 50, 75 and 100), inclination angles ($\Phi = 0^\circ, 45^\circ, 90^\circ$ and 135°), the ratio of the size of the heating element to the enclosure width ($\varepsilon = 0.4$, 0.6 and 0.8) and Rayleigh number (Ra $=$ 10^4, 10^5 and 10^6). For constant values of ($\varepsilon = 0.4$, 0.6 and 0.8) and (Ra $=$ 10^4, 10^5 and 10^6) respectively, the increase of Hartmann number for constant value of inclination angle does not have a significant effect on the vortices number, but only a slight effect on the vortices shape. This is because the increase in inclination angle will increase the buoyancy force and reduces the Hartmann number effect. From the other hand, the increase in the Rayleigh number increases Nusselt number and causes to increase the heat transfer rate, while increasing of ε decreases the heat transfer rate and Nusselt number. It can be also observed from the same figures that the increase in both the ratio of the size of the heating element to the enclosure width (ε) and Rayleigh number create a large core vortex that

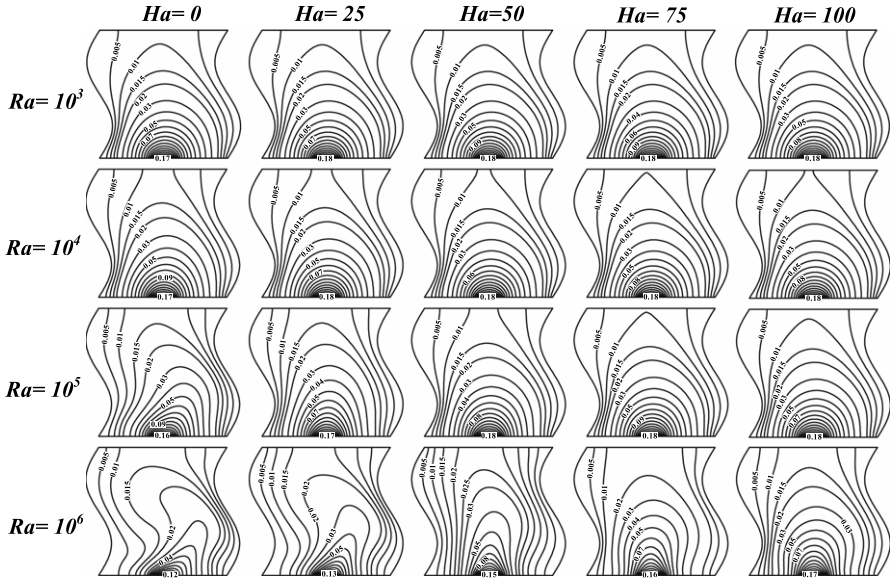

Fig. 5. Isotherms for different Hartmann numbers (Ha) and Rayleigh numbers (Ra) with $\varepsilon = 0.2$ and $\Phi = 0^\circ$.

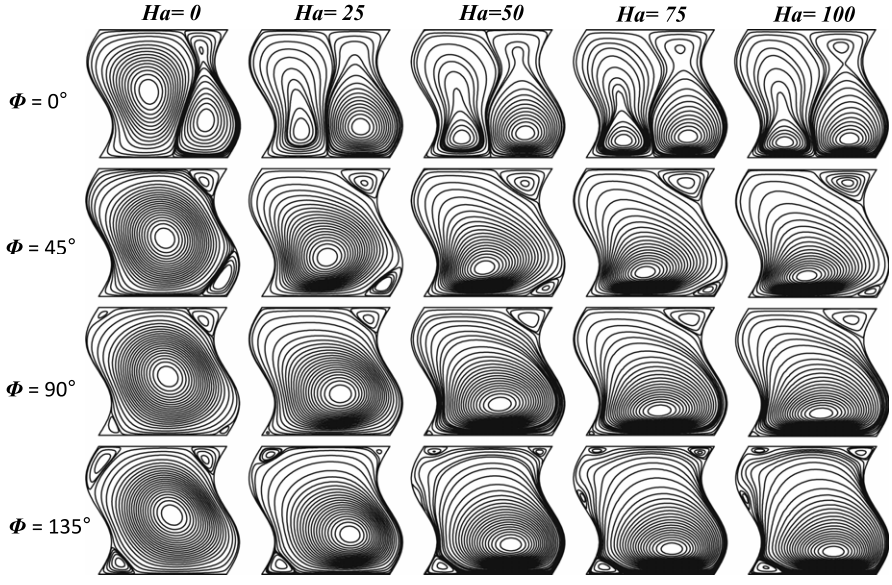

Fig. 6. Streamlines for different Hartmann numbers (Ha) and inclination angles (Φ) with $\varepsilon = 0.4$ and $\mathrm{Ra} = 10^4$.

controls the flow field inside the enclosure. The core of vortices moves into the bottom wall where the heat source exists and the vortices shape changes from the circular shape to elliptical one, and the large axis direction of the elliptical center is parallel to the direction of the magnetic field. For constant values of the Hartmann number, the increase in the inclination angles ($\Phi = 45^\circ$–135°) does not have a significant effect since the magnetic field effect decreases. Except for ($\Phi = 0^\circ$), the increase in the Hartmann number leads to produce two vortices that control the flow field inside the enclosure. This is due to symmetrical boundary conditions and the magnetic field plays a good role in flow field damping especially for high value of Hartmann number ($\mathrm{Ha} = 100$). For ($\varepsilon = 0.6$ and 0.8) and ($\mathrm{Ra} = 10^5$ and 10^6) respectively, the streamlines have approximately the same behavior as it noticed for ($\varepsilon = 0.4$) and ($\mathrm{Ra} = 10^4$).

About isothermal lines, (Figs. 7, 9 and 11), the increase in the Hartmann number for constant values of Φ, ε and Ra, does not greatly increase the values of isotherm lines and reduce the temperature oscillations. The isothermal lines take approximately symmetrical shape especially for large value of Hartmann number ($\mathrm{Ha} = 100$). From the other side, the isothermal lines are slightly affected by Hartmann number except for ($\Phi = 0$). This is due to the reason that the magnetic field is high especially for small values of ($\varepsilon = 0.4$) and ($\mathrm{Ra} = 10^4$). But with increasing the ε (from 0.6 to 0.8) and Rayleigh number (from 10^5 to 10^6), the isothermal lines are greatly affected by increasing of Hartmann number especially

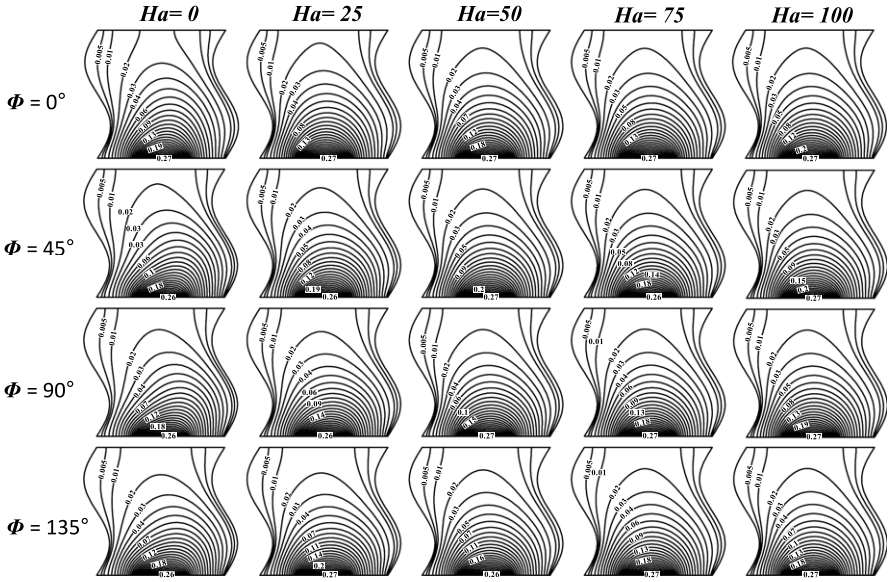

Fig. 7. Isotherms for different Hartmann numbers (Ha) and inclination angles (Φ) with $\varepsilon = 0.4$ and Ra $= 10^4$.

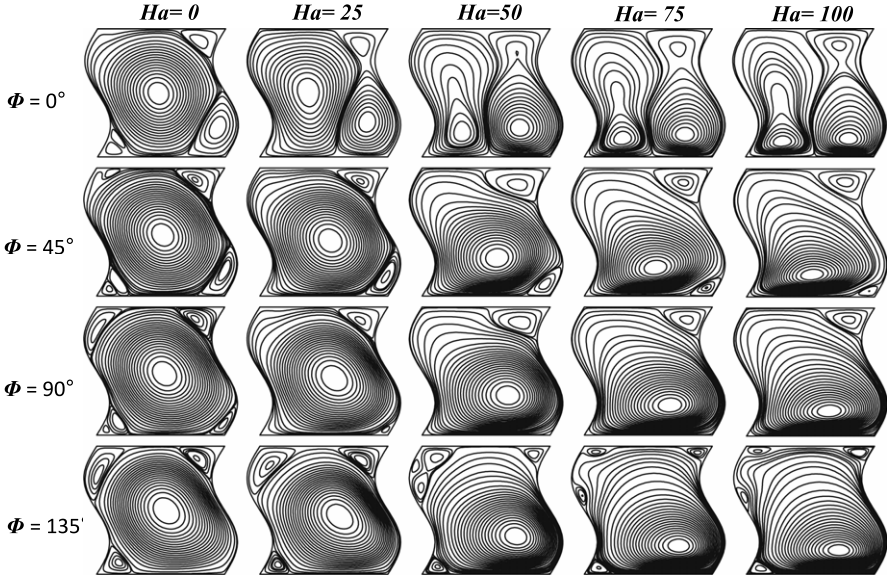

Fig. 8. Streamlines for different Hartmann numbers (Ha) and inclination angles (Φ) with $\varepsilon = 0.6$ and Ra $= 10^5$.

for ($\varepsilon = 0.8$) and (Ra $= 10^6$). For (Ha $= 0$), the isothermal lines inside the enclosure become more confused since the convection effect becomes strong, but with increasing of Hartmann number (Ha $= 25$–100), the convection effect reduces due to increase in the magnetic field role. The increasing of the Hartmann number increases the values of the isothermal lines adjacent the heat source. This is because the magnetic field damps the temperature and the heat transfer rate adjacent the heat source position.

In Figs. 12–15, the increase in the Hartmann number decreases the value of Nusselt number. This is because the increase in the Hartmann number damps the heat transfer rate and flow field, leading to reduce the value of Nusselt number. It can be observed that the Nusselt number firstly increases with increasing inclination angles and then decreases for all values of Hartmann number. The increase in inclination angles ($0^\circ \leq \Phi \leq 45^\circ$) increases Nusselt number, because the buoyancy force in y-direction that resisting the magnate field is large. When the inclination angles in the range ($45^\circ \leq \Phi \leq 90^\circ$) no important effect can be detected on the Nusselt number because the buoyancy force that assists the flow and the magnetic effect that damps the flow are approximately equal. When the inclination angles in the range ($90^\circ < \Phi \leq 135^\circ$) the buoyancy force works together with the magnetic effect to damp the flow field inside the enclosure leading to reduce the Nusselt number. Also, it can be noticed from Figs. 12–15 that the increase in the Rayleigh number increases the Nusselt

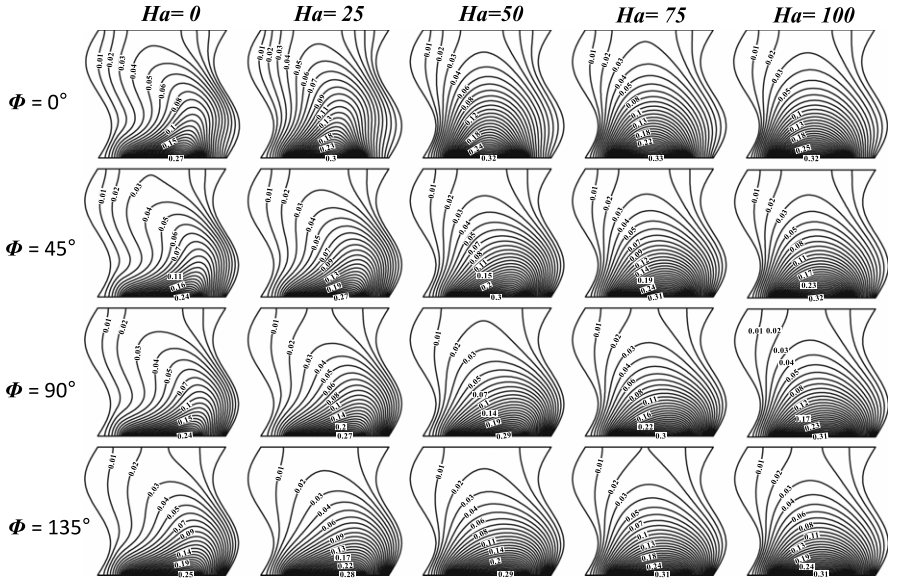

Fig. 9. Isotherms for different Hartmann numbers (Ha) and inclination angles (Φ) with $\varepsilon = 0.6$ and $\mathrm{Ra} = 10^5$.

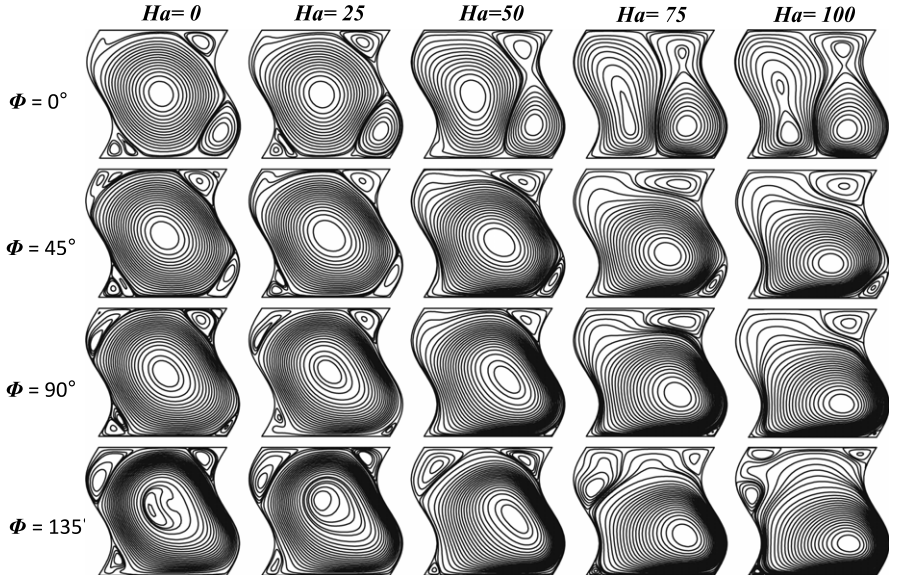

Fig. 10. Streamlines for different Hartmann numbers (Ha) and inclination angles (Φ) with $\varepsilon = 0.8$ and $\mathrm{Ra} = 10^6$.

number because the increase in Rayleigh number increases the heat transfer rate. But the increase in the ratio of the size of the heating element to the enclosure width (ε) reduces the Nusselt number due to reduction in the convection heat transfer by increasing the viscous force that acts against the buoyancy force. Finally, four correlation equations of average Nusselt number have been predicted depending on variation in Rayleigh number, enclosure inclination angle and Hartmann number for various values of (ε) by using least square method. These correlations can be presented as follows:-

For $0^\circ \leq \Phi \leq 135^\circ$, $10^3 \leq \mathrm{Ra} \leq 10^6$, $0 \leq \mathrm{Ha} \leq 100$

$$\varepsilon = 0.2$$

$$\overline{Nu} = 6.707 + 2.8 \times 10^{-6}\mathrm{Ra} - 0.013\mathrm{Ha} + 0.001\Phi \tag{9}$$

the maximum correlation coefficient or residual = **0.896**

$$\varepsilon = 0.4$$

$$\overline{Nu} = 5.438 + 2.8 \times 10^{-6}\mathrm{Ra} - 0.019\mathrm{Ha} + 0.001\Phi \tag{10}$$

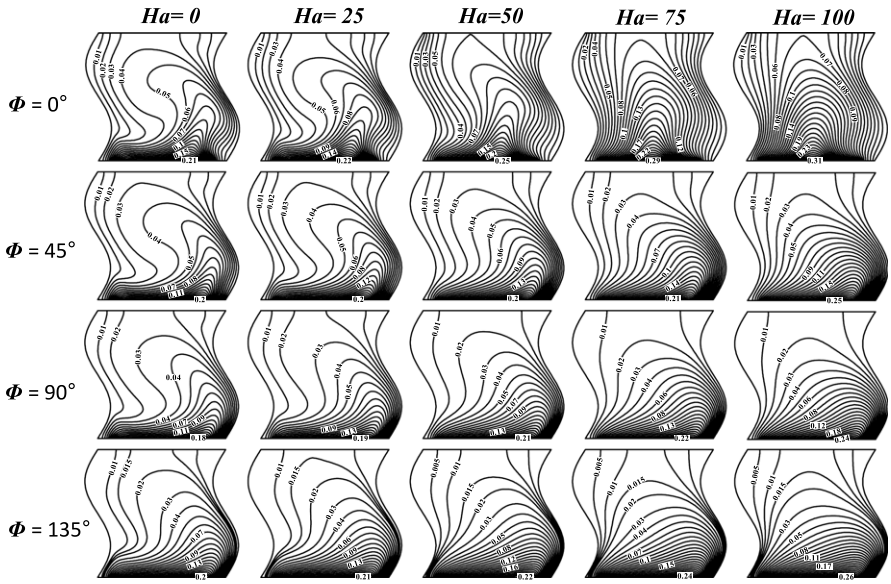

Fig. 11. Isotherms for different Hartmann numbers (Ha) and inclination angles (Φ) with $\varepsilon = 0.8$ and Ra $= 10^6$.

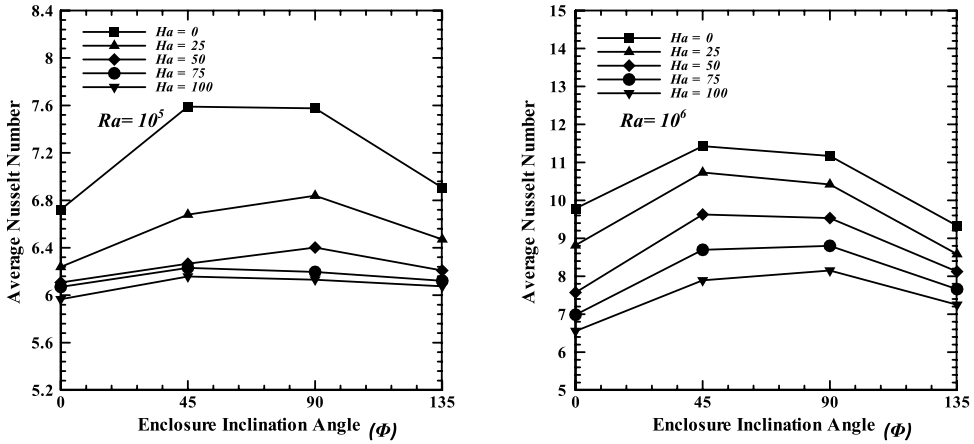

Fig. 12. Variation of the average Nusselt numbers along the heated surface (Nu_l) with different enclosure inclination angles (Φ) and Hartmann numbers (Ha) for Ra $= 10^5$ (on the left) and Ra $= 10^6$ (on the right) at $\varepsilon = 0.2$.

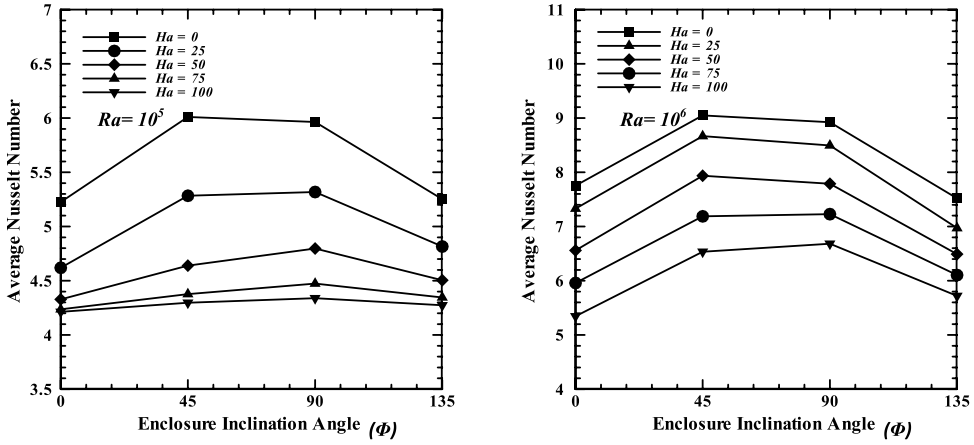

Fig. 13. Variation of the average Nusselt numbers along the heated surface (Nu_l) with different enclosure inclination angles (Φ) and Hartmann numbers (Ha) for Ra $= 10^5$ (on the left) and Ra $= 10^6$ (on the right) at $\varepsilon = 0.4$.

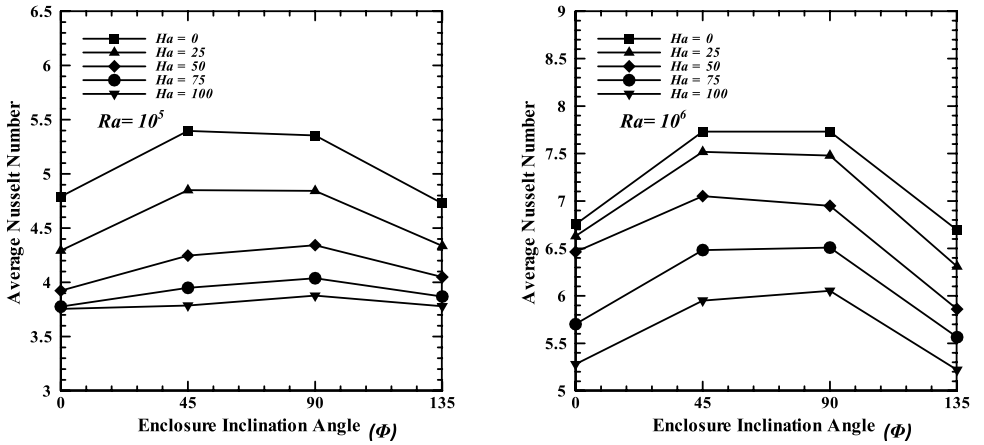

Fig. 14. Variation of the average Nusselt numbers along the heated surface (Nu_l) with different enclosure inclination angles (Φ) and Hartmann numbers (Ha) for Ra $= 10^5$ (on the left) and Ra $= 10^6$ (on the right) at $\varepsilon = 0.6$.

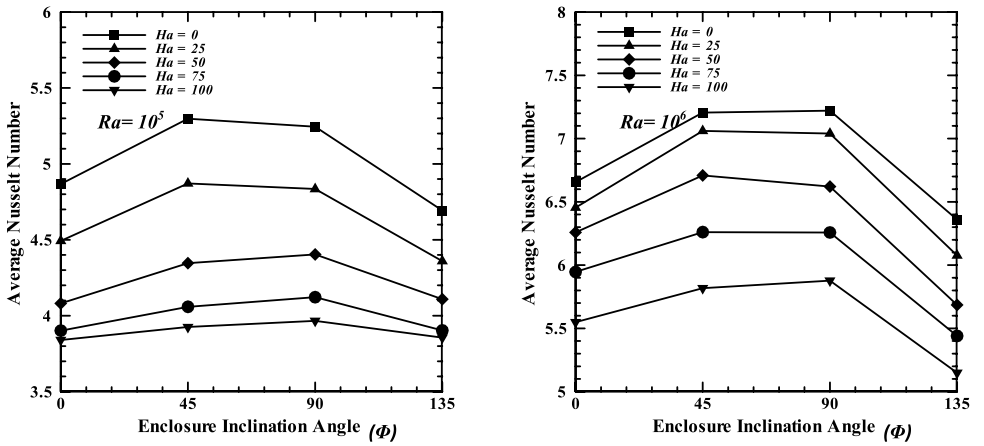

Fig. 15. Variation of the average Nusselt numbers along the heated surface (Nu_l) with different enclosure inclination angles (Φ) and Hartmann numbers (Ha) for Ra $= 10^5$ (on the left) and Ra $= 10^6$ (on the right) at $\varepsilon = 0.8$.

the maximum correlation coefficient or residual = **0.945**

$$\varepsilon = 0.6$$
$$\overline{Nu} = 4.852 + 2.5 \times 10^{-6}\mathrm{Ra} - 0.016\mathrm{Ha} + 0.001\Phi \tag{11}$$

the maximum correlation coefficient or residual = **0.965**

$$\varepsilon = 0.8$$
$$\overline{Nu} = 4.875 + 2.2 \times 10^{-6}\mathrm{Ra} - 0.013\mathrm{Ha} - 0.002\Phi \tag{12}$$

the maximum correlation coefficient or residual = **0.975**

To ensure that these approximation correlations are usable, the maximum correlation coefficient or residual had been obtained for each equation as mentioned above. The minimum value of the maximum correlation coefficient is (**0.896**), which means that these approximate correlations are good for predicting the value of average Nusselt number.

7. Conclusions

The longitudinal magnetic field and discrete isoflux heat source size effects on the natural convection flow inside a tilted sinusoidal corrugated enclosure for different enclosure inclination angles are analyzed and solved numerically by using finite volume method. A wide range of parameters are used in the present analysis (Hartmann numbers (0, 25, 50, 75 and 100), Rayleigh numbers (10^3, 10^4, 10^5 and 10^6), ($\varepsilon = 0.2$, 0.4, 0.6 and 0.8) and inclination angles ($\Phi = 0°$, 45°, 90° and 135°)). Some of important conclusions drawn from the present analysis, are as follows:

- The magnetic field damps the flow and the temperature oscillations by reducing the fluid velocity and Nusselt number. For large values of the Hartmann number, the isothermal lines move toward the vertical sidewall and divided into two symmetrical isothermal lines. For small values of Rayleigh number ($Ra = 10^3$–10^4) the isothermal lines are appear to be symmetrical.
- For streamlines at $\varepsilon = 0.2$, $\Phi = 0^\circ$ and $Ha = 0$ and low values of Ra (10^3–10^4), two large vortices appear on the left and right sidewalls of the enclosure, but with increasing Ra (10^5–10^6), a large left vortex will appear only which controls the flow inside the enclosure, while the right vortex is reduced in size and divided into minor vortices located near the top and bottom of the right vertical wall.
- The magnetic field effect depends strongly upon the inclination angle. The effect of the magnetic field on the streamlines is very significant for ($\Phi = 0^\circ$) and for all values of Rayleigh number ($Ra = 10^3$–10^4). This effect will decrease with the increase in inclination angles ($\Phi > 0^\circ$) especially for large value of Rayleigh number ($Ra = 10^6$).
- The core of vortices strongly depends on the magnetic field (magnitude and direction). Also, the increase in the value of the magnetic field moves the vortices core into the bottom wall where the heat source exists, and also changes the shape of vortices core from the circular shape to elliptical one, and the direction of the large axis of the elliptical center will be parallel to the direction of the magnetic field effect.
- The isothermal lines are affected slightly by inclination angles especially for small values of ($\varepsilon = 0.2$) and ($Ra = 10^3$).
- Nusselt number firstly increases with increasing inclination angles and then decreases for all values of Hartmann number. The increase in inclination angles ($0^\circ \leq \Phi \leq 45^\circ$) increases Nusselt number. For inclination angles ($45^\circ \leq \Phi \leq 90^\circ$) Nusselt number will not be affected largely. For ($90^\circ < \Phi \leq 135^\circ$) Nusselt number decreases.
- The increase in the (ε) decreases the Nusselt number and then decreases convection heat transfer effect.
- Four mathematical correlations are proposed which can used to accurately predict the average Nusselt number for each (ε) in terms of Rayleigh number, Hartmann number and enclosure inclination angle.

References

[1] J.M. Jalil, K.A. Al-Tae'y, MHD turbulent natural convection in a liquid metal filed square enclosure, Emirates J. Eng. Res. 12 (2007) 31–40.
[2] J.S. Walker, B.F. Picologlou, Liquid metal flow in insulating rectangular expansion with a strong magnetic field, J. Fluid Mech. 305 (1995) 111–126.
[3] J. Baumgartl, A. Hubert, G. Muller, The use of magneto hydrodynamic effects to investigate fluid flow in electrically conducting melts, Phys. Fluids A-5 (12) (1993) 3280–3289.
[4] J. Baumgartl, G. Muller, Calculation of the effects of magnetic field damping on fluid flow: comparison of magneto hydrodynamic models of different complexity, in: Proceedings Eight European Symposium on Materials and Fluid Sciences in Microgravity, Brussels, Belgium, 1992, pp. 161–164.
[5] L.S. Yao, Natural convection along a wavy surface, Trans. ASME, J. Heat Transfer 105 (1983) 465–468.
[6] L. Adjlout, O. Imine, A. Azzi, M. Belkadi, Laminar natural convection in an inclined cavity with a wavy wall, Int. J. Heat Mass Transfer 45 (2002) 2141–2152.
[7] C.C. Wang, C.K. Chen, Forced convection in a wavy-wall channel, Int. J. Heat Mass Transfer 45 (2002) 2587–2595.
[8] H.M. Metwally, R.M. Manglik, Enhanced heat transfer due to curvature-induced lateral vortices in laminar flows in sinusoidal corrugated-plate channels, Int. J. Heat Mass Transfer 47 (2004) 2283–2292.
[9] N. Kruse, P.R. Von Rohr, Structure of turbulent heat flux in a flow over a heated wavy wall, Int. J. Heat Mass Transfer 49 (2006) 3514–3529.
[10] X.B. Chen, P. Yu, S.H. Winoto, H.T. Low, Free convection in a porous cavity based on the Darcy–Brinkman–Forchheimer extended model, Numer. Heat Transfer A 52 (2007) 377–397.
[11] G. Comini, C. Nonino, S. Savino, Effect of aspect ratio on convention enhancement in wavy channels, Numer. Heat Transfer A 44 (2003) 21–37.
[12] P.K. Das, S. Mahmud, Numerical investigation of natural convection inside a wavy enclosure, Int. J. Therm. Sci. 42 (2003) 397–406.
[13] A. Dalal, M.K. Das, Laminar natural convection in an inclined complicated cavity with spatially variable wall temperature, Int. J. Heat Mass Transfer 48 (2005) 3833–3854.
[14] Y. Varol, H.F. Oztop, Effects of inclination angle on natural convection in wavy solar air collectors: a computational modeling, in: The 2nd International Green Energy Conference, UOIT, Oshawa, Canada, 2006.
[15] S.H. Hussain, R.N. Mohammed, Effects of out of phase and inclination angles on natural convection heat transfer flow of air inside a sinusoidal corrugated enclosure with spatially variable wall temperature, J. Enhanc. Heat Mass Transfer 18 (5) (2011) 403–417.
[16] N.M. Al-Najem, K.M. Khanafer, M.M. El-Refaee, Numerical study of laminar natural convection in tilted enclosure with transverse magnetic field, Internat. J. Numer. Methods Heat Fluid Flow 8 (1998) 651–672.
[17] P. Kandaswamy, S. Malliga, N. Nithyadevi, Magnetoconvection in an enclosure with partially active vertical walls, Int. J. Heat Mass Transfer 51 (2008) 1946–1954.
[18] M. Pirmohammadi, M. Ghassemi, G.A. Sheikhzadeh, Effect of magnetic field on buoyancy driven convection in differentially heated square cavity, IEEE Trans. Magn. 45 (2009) 407–411.
[19] H. Ozoe, K. Okada, The effect of the direction of the external magnetic field on the three-dimensional natural convection in a cubic enclosure, Int. J. Heat Mass Transfer 32 (1989) 1939–1953.
[20] J.M. Jalil, T.K. Murtadha, K.A. Al-Tae'y, Three-dimensional computation of turbulent natural convection in the presence of magnetic field, J. Indian Inst. Sci. 86 (2006) 705–721.
[21] M. Syou, T. Tagawa, H. Ozoe, Average heat transfer rates measured and numerically analyzed for combined convection of air in an inclined cylindrical enclosure due to both magnetic and gravitational fields, Exp. Therm Fluid Sci. 27 (2003) 891–899.
[22] M. Pirmohammadi, M. Ghassemi, Effect of magnetic field on convection heat transfer inside a tilted square enclosure, Int. Commun. Heat Mass Transfer 36 (2009) 776–780.
[23] G. Saha, Finite element simulation of magnetoconvection inside a sinusoidal corrugated enclosure with discrete isoflux heating from below, Int. Commun. Heat Mass Transfer 37 (2010) 393–400.
[24] M. Ece, E. Buyuk, Natural convection flow under a magnetic field in an inclined square enclosure differentially heated on adjacent walls, Meccanica 42 (2007) 435–449.
[25] S. Saha, T. Sultana, G. Saha, M.M. Rahmann, Effect of discrete isoflux heat source size and angle of inclination on natural convection heat transfer inside a sinusoidal corrugated enclosure, Int. Commun. Heat Mass Transfer 35 (2008) 1288–1296.
[26] J. Ferzinger, M. Peric, Computational Methods for Fluid Dynamics, 2nd ed., Springer Verlag, Berlin, Hedelberg, 1999.
[27] B.D. Thompson, F.C. Thames, F. Mastin, Automatic numerical generation of body-fitted curvilinear co-ordinate system, J. Comput. Phys. 15 (1974) 299–319.
[28] H.L. Stone, Iterative solution of implicit approximations of multidimensional partial differential equations, SIAM J. Numer. Anal. 5 (1968) 530–558.
[29] S.V. Patankar, Numerical Heat Transfer and Fluid Flow, Hemisphere Publishing Corporation, New York, 1980.